Novel-m2866-5p and miR8181-x are involved in the regulation of aureochrome and photosynthesis in Saccharina japonica

Xiaoqi Yang
IOCAS https://orcid.org/0000-0003-1635-7285
Delin Duan (dlduan@qdio.ac.cn)
https://orcid.org/0000-0001-5356-5839

Research article

Keywords: miR8181, aureochrome, PGR5, competing endogenous RNA, photo-protection

Posted Date: November 18th, 2019

DOI: https://doi.org/10.21203/rs.2.17391/v1

Abstract

Background: Aureochrome, a blue-light receptor only in photosynthetic stramenopiles, plays an important role in algal growth and development. Previous researches have reported that aureochrome is involved in the photoacclimation, cell division and sex organ development. It holds reversed effector-sensor topology for the reception of blue light, acting as the candidate of optogenetic tools in transcription regulation. However, the inner regulatory mechanism of aureochrome is still unclear. In this study, we explored the expression profiles of microRNAs (miRNAs) and mRNAs, aiming to construct the regulatory network between miRNAs and aureochrome.

Results: Our results showed that 18 identified miRNAs have potential aureochrome regulatory function. Among the screened microRNAs, both novel-m2866-5p and miR8181-x exhibited a negative correlation with Aureochrome5. The transcription of novel-m2866-5p and miR8181-x exhibited tissue specificity, indicating that these two microRNAs might function in different tissues. Moreover, miR8181-x could regulate kelp growth, while novel-m2866-5p was possibly involved in the arginine metabolic pathway. Aureochrome5 and photosynthetic genes exhibited similar expression trends, suggesting coordination between photosynthesis and blue light receptors. Moreover, the proton gradient regulation 5 (PGR5), which functions in the induction of energy-dependent quenching, exhibited a co-expression pattern with Aureochrome5. These patterns were further observed upon incubation with N,N'-dicyclohexylcarbodiimide (DCCD), which exhibited up-regulation of both PGR5 and Aureochrome5 and confirmed their endogenous competition.

Conclusion: Our study revealed that both novel-m2866-5p and miR8181-x were involved in the regulation of aureochrome, and that miR8181-x could act as a bridge between blue light receptors and photosynthesis in kelp.

Background

Light serves as a biological stimulus that triggers signal transduction pathways via a specific photoreceptor. The responses of photoreceptors to dynamic changes in the wavelength, direction and duration of light illumination are important for seaweed growth and development (Jiao et al. 2007; Masuda et al. 2008; Jaubert et al. 2017). Following the absorption of light energy, photosynthetic antenna pigments act as a driving force for photosynthesis, which triggers the splitting of H_2O and regeneration of NADPH by the electron transport chain (Nixon and Mullineaux, 2001). The association between photoreceptor and photosynthesis has been elucidated in the green alga *Chlamydomonas reinhardtii* (Petroutsos et al. 2016; Allorent et al. 2017). Blue light receptors (phototropins) control energy-dependent non-photochemical quenching (qE) by inducing light-harvesting complex stress-related protein 3 (LHCSR3) expression under high light intensity(Petroutsos et al. 2016). Induction of the expression of a UV photoreceptor (ultra-violet resistance locus 8, UVR8) on LHCSR1 and photosystem II subunit S (PsbS) has been documented (Heijde and Ulm, 2013; Allorent et al. 2017). These studies revealed that both phototropins and UVR8 can protect green algae from over-reduction in electron transport chain.

Similar to the primary symbiosis exhibited by green algae, photosynthetic stramenopiles acquire the blue light responses of phototropism, chloroplast photorelocation, and photomorphogenesis from secondary symbiosis (Matiiv and Chekunova, 2018). Aureochrome is new type of blue light receptor in this clade, belonging to the species *Vaucheria frigida* (Takahashi et al. 2007). Aureochrome consists of a basic region/leucine zipper (bZIP) domain at the N-terminus and a light-oxygen-voltage (LOV) domain at the C-terminus. SjAUREO from the brown alga *Saccharina japonica* was shown to share 40%–92% sequence similarity with other photosynthetic stramenopiles (Deng et al. 2014). Yeast two-hybrid screening further proved the strong interaction between SjAUREO and the light-harvesting complex (LHC) in *S. japonica* (Luan et al. 2019), indicating that photosynthesis and aureochrome are associated at the protein level. Moreover,PtAUREO1a and PtAUREO1b mutants exhibit significantly decreased photosynthetic potential in *Phaeodactylum tricornutum* (Coasta et al. 2013; Mann et al. 2017). However, details regarding the association between aureochrome and photosynthesis remain to be further explored.

MicroRNAs (miRNAs) play an important role in post-transcriptional gene regulation via base paring with their complementary sequences (Bartel, 2004; Voinnet, 2009). Tarver et al. (2015) noted that the miRNAs in brown algae have evolved independently with five other eukaryotic lineages: animals, land plants, chlorophyte green algae, demosponges and slime moulds. The developmental plasticity mediated by miRNAs allows plants to efficiently cope with environmental stress (Song et al. 2019). A previous study reported that mature miRNAs participate in the red light signalling pathway to regulate plant photomorphogenesis (Sun et al. 2018).

Although miRNAs from the lineage of brown algae have been identified (Cock et al. 2010), the interaction of miRNAs with algal photoreceptors is unclear. Additionally, competing endogenous RNAs (ceRNAs) that share the common miRNA response element can reduce miRNA activity, leading to the derepression of specific mRNAs (Gupta, 2014). Therefore, it is important to explore the influence of the miRNA regulatory network on aureochrome in brown algae.

Incubation in low tidal zone inhabitants with blue light irradiance, light reception and subsequent signal amplification are crucial for the development and growth of *S. japonica.* Through analysis of mRNA and miRNA data, we aimed to explore the relationship between miRNA and *aureochrome,* to verify the associated miRNAs and to examine the function of these miRNAs in the regulation of the blue light receptor followed by photosynthesis. Our study will be aid the understanding of the role of miRNAs in the regulation of kelp growth and development.

Results

Identification of miRNAs that targeted aureochromes

By conducting a high-throughput mRNA array to test the response of *S. japonica* to light quality, we screened five homologous sequences that encoded aureochrome. In addition to *Aureochrome3,* the remaining four homologs were upregulated in response to blue light (BL) (Fig. 1). Based on the complementarity interactions between miRNAs and target genes, we made homology predictions for the miRNA target genes with Patmatch (v1.2) software. In turn, we obtained 18 miRNA sequences targeting a*ureochromes (*Table. 1), constructing one miRNA-*aureochrome* network (Fig. 2). The two candidate miRNAs, namely, *miR8181-x* and *novel-m2866–5p,* targeted *Aureochrome5* with high fidelity (Fig. 3). The conserved miRNA *miR818-x,* 18 nt in length, was classified into the miR8181 family. The newly identified *novel-m2866–5p* with 20 nt exhibited stem loop structures (Fig. S1), and both *miR8181-x* and *novel-m2866–5p* were down-regulated in response to BL, which was the opposite to the result obtained for *aureochrome5* (Table. 2).

qRT-PCR analysis of *miR8181-x* and *novel-m2866–5p* showed that these two miRNAs were negatively correlated with *aureochrome5 (*Fig. 4), and the transcription levels of these miRNAs were significantly higher in the kelp blade than in the holdfast, whereas the *Aureochrome5* transcription patterns were the opposite.

Cluster analysis of the miRNA target genes

In total, 1915 sequences and 31 mRNAs were screened as potential targets of *miR8181-x* and *novel-m2866–5p,* respectively. According to these transcription patterns, we separately grouped these genes by hierarchical clustering. The target genes of *novel-m2866–5p* were grouped into 4 clusters, and those from cluster 1 was significantly up-regulated in response to BL (Fig. 7). In cluster 1, *Kif6* exhibited a similar trend as *Aureochrome5.* To further screen the related target sequences of *miR818-x,* a total of 1915 sequences were classified into 6 clusters based on their degrees of transcription using TCseq. There were 311 genes (including *PsbO,* cluster 4) that were significantly up-regulated in response to BL than dark and WL conditions (Fig. 8). Moreover, we conducted GO and KEGG analysis to target sequences in cluster 4, and functional analysis indicated high transcription levels of sequences associated with kelp growth, establishment of localization, cytoplasmic transport, photosynthesis, ubiquitin-mediated proteolysis, RNA transport, and carbon fixation (Fig. 9).

Functional prediction of objective miRNAs

We used DAVID to determine the KEGG and GO pathway for biological analysis of target genes. The results showed that *miR8181-x was* possibly involved in the cellular component category, with the enriched terms “organelle”, “cell part”, “macromolecular complex” and “membrane”. In the molecular function (MF) category, “binding” and “catalytic activity”, and “molecular function regulator” were significantly enriched (Fig. 10a). In the biological process (BF) category, “metabolic process”, “cellular process”, “single-organism process”, “localization”, “response to stimulus”, and “developmental process” were significantly enriched. KEGG pathway analysis revealed that the top three pathways were glycolysis, cyanoamino acid metabolism, and biosynthesis of amino acids (Fig. 10b). The number of target sequences of *novel-m2866–5p* was lower than that of *miR8181-x.* GO analysis results showed that “metabolic process”, “cellular process”, and “single-organism process” were the three most common BP terms and the most highly enriched MF terms were “binding” and “catalytic activity” (Fig. 11).

ceRNA network construction and functional analysis

Based on the target analysis, we further screened the negative-correlation pairs between the miRNAs and mRNAs. A total of 311 sequences and 4 mRNAs were screened as the potential ceRNAs of *miR8181-x* and *novel-m2866–5p,*respectively (Fig. 12a). Functional analysis of these ceRNAs indicated that they were involved in metabolic pathways, biosynthesis of secondary metabolites and carbon metabolism (Fig. 12b). Moreover, the *proton gradient regulation 5 (PGR5),* which played an important role in metabolic pathways, was also screened and can be regarded as one of the potential ceRNAs of *Aureochrome5.*

Dynamic transcript regulation of photosynthetic electron transport

In response to BL, *PsaA* and *PsaD* in the photosystem I, *PetA* and *PetD* in the cytochrome b6/*f* complex, and ATP synthase were up-regulated, but *PsbA* and *PsbB* in photosystem II were down-regulated (Fig. S2a). In addition to *PsbA* and *PetA,* the transcription patterns under WL coincided with those under BL (Fig. S2b).

Effect of DCCD on the photosynthetic ability of *S. japonica*

During cultivation under WL and BL, the non-photochemical quenching (NPQ) index was significantly increased. After adding N,-N'-dicyclohexylcarbodiimide (DCCD), NPQ was down-regulated under BL, which was accompanied by a decrease in qE (Fig. 13, 14). The decrease in NPQ was also consistent with the decrease of *F*v/*F*m and Rfd, which indicated the decrease of photosynthetic capacity. Additionally, the transcription of *PGR5* was up-regulated under BL, and *Aureochrome5* exhibited a co-expression pattern with *PGR5* (Fig. 15).

Discussion

By integration analysis of the miRNA and mRNA data, we found that there were 18 candidate miRNAs that targeted *aureochrome* orthologs. Both *Aureochrome1* and *Aureochrome5* had different miRNA-binding sites, indicating their complex regulatory network. Among the candidate miRNAs, the level of novel miRNAs was significantly higher than that of known miRNAs. The high amount of novel miRNAs in brown algae was attributed to the rapid evolution process (Cock et al. 2017).

Usually, miRNA can splice or cleave the RNA strand at the binding site by guiding the RNA-induced silencing complex and, thus, the transcription of miRNA is negatively correlated with targeted gene transcription (Denzler et al. 2014). In our study, the conserved miRNA *miR8181-x* and novel miRNA *novel-m2866–5p* were negatively associated with *aureochrome5* in response to light irradiation. The differential expression of these two miRNAs in the blade and holdfast indicated their complex and independent roles in kelp tissue. Due to the vertical cultivation of kelp, the holdfast is closer to the sea surface than the other part of the blade. The high transcription level of *aureochrome5* in the holdfast indicated the rapid response to increased light irradiation.

In addition to *Aureochrome5, novel-m2866-5p* and *miR8181-x* were presumed to target 30 and 1914 gene sequences, respectively. A small number of target genes of *novel-m2866–5p* revealed significant enrichment of KEGG pathways associated with arginine metabolic processes. In green plants, the *miR8181* family is involved in anthocyanin biosynthesis (Sun et al. 2017). KEGG pathway analysis of the *miR8181-x* target genes revealed that the genes were mainly involved in glycolysis/gluconeogenesis for energy supply. GO enrichment analysis indicated that the most common processes are cell differentiation, cell cycle and cell development, indicating the involvement of *miR8181-x* in the regulation of growth and development in *S. japonica.*

BL promotes the growth of *S. japonica* sporophytes through photosynthetic processes (Wang et al. 2010; Deng et al. 2012). Among the photosynthetic electron transport components, PSII is the most sensitive site of the photosynthetic electron transport chain in the response to environment interference (Chen et al. 2016). In our study, both the *PsbA* and *PsbB* PSII subunits were down-regulated, indicating the inhibition of PSII activity. These results are also consistent with the reversible decrease in PSII quantum yield, which may an effective approach to increase the photoprotection capacity via a rapid increase in NPQ. Therefore,the kelpcan sufficiently cope with BL and resist the damage caused by excess light. Moreover, the manganese-stabilizing protein *PsbO* in the oxygen-evolving complex exhibited a similar expression trend as *Aureochrome5.* An increase in PsbO levels could cause the splitting of H_2O to oxygen and protons and provide electrons for the photosynthetic electron chain (PET), contributing to the occurrence of photosynthesis. Therefore, kelp can coordinate association aureochromes and photosynthesis in response to irradiation.

In this study, *PGR5* was identified to compete for the common response element of *miR8181-x* with *Aureochrome5,* suggesting the ceRNA relationship between *PGR5* and *Aureochrome5.* PGR5 could induce thermal dissipation by adjusting the production of the

trans-membrane proton gradient, and the absence of the PGR5 protein in chloroplasts could inhibit NPQ occurrence (Kawashima et al. 2017; Sato et al. 2018). Upon cultivation with DCCD, NPQ was significantly down-regulated by a decrease in pH-regulated energy dissipation, leading to the decease in photo-protection capacity. Moreover, *Aureochrome5* was also up-regulated and exhibited co-expressions with PGR5, thus confirming their ceRNA relationship. Therefore, we speculated that *miR818-x* may act as a bridge to contribute to the coordination between photosynthesis and the blue-light receptor aureochrome.

Conclusions

MiR8181-x and *novel-m2866–5p* negatively regulate *Aureochrome5* in a tissue specific manner. *miR8181-x* functions in the regulation of cell differentiation, cell cycle and cell development and plays an important role in kelp growth. The enhancement of *Aureochrome5* under BL irradiation was coordinated with kelp photosynthesis and photoprotection. *PGR5* incorporates the ceRNAs of *Aureochrome5,* and might act as the switch between the regulation of photo-protection and Aureochrome.

Methods

Sample collection and treatment

The *S. japonica* juvenile sporophytes (“Zhongke no. 1”) were identified through appearance by us and collected from experimental aquaculture area in Rongcheng, Shandong, China. After washing the epiphytes thoroughly with sterilized seawater, the kelps were stored in cold conditions during the shipping. The kelps were pre-cultured in the dark at 10 °C for 24 h and then treated with darkness, white light (WL), or BL for 3 h. White fluorescent lamps (Philips, Shanghai, China) and blue light-emitting diodes (460~475 nm wavelengths; Ichia, Japan) were applied as light sources. DCCD (final concentration 40 μM) was added to the culture medium before exposure to light irradiation. After treatment, the sporophytes were rapidly frozen with liquid nitrogen and then stored at −80 °C for subsequent RNA extraction. “Zhongke no. 1” was originally cultivated after 9 generations of hybridization with long and wide phenotypes *S. japonica.* A voucher specimen of *S. japonica* was deposited in the Resource-sharing Platform of Specimens Marine Biological Museum Chinese Academy of Sciences (No. MBM436715).

RNA isolation and library preparation.

Total RNA was isolated using TRIzol reagent (Invitrogen, CA, USA). The extracted RNA was qualitatively examined by 1% agarose gel electrophoresis, and the concentration was determined by a Nanodrop 2000 spectrophotometer (Thermo Scientific, Wilmington, USA). After extraction, the RNAs, with molecules weights ranging from 18 to 30 nt, were separated by 15% polyacrylamide gel electrophoresis (PAGE). Then, the 3’ adapters were added, and the 36–44 nt RNAs were enriched. Subsequently, the 5’ adapters were ligated to the RNAs. The ligation products were reverse transcribed and the 140–160 bp PCR products were enriched to generate a cDNA library. Finally sequencing was conducted on an Illumina HiSeqTM 2500 at Gene Denovo Biotechnology Co. (Guangzhou, China). The RNA integrity and concentration were further measured using an Agilent 2100 Bioanalyzer (Agilent Technologies, CA, USA). The small RNA and mRNA were reverse transcribed to cDNA and then sequenced with a HiSeq 2500 and HiSeq 4000 (Illumina, San Diego, CA, USA), respectively.

Identification of miRNAs and target gene prediction

After removing reads containing adapters or low-quality bases, all of the clean tags were aligned with small RNAs in the Rfam and GenBank databases (Release 209.0), and our previous *S. japonica* genome data were registered in the NCBI database (accession: MEHQ00000000). The rRNA, scRNA, snoRNA, snRNA and tRNA sequences were filtered out. All of the clean tags were validated using the miRBase database with known miRNAs. We selected the following prediction criteria for novel miRNAs: length, 18–25 nt; maximal free energy allowed for a miRNA precursor, 18 kcal/mol; space between miRNA and miRNA*, 14–35 nt; maximal asymmetry of miRNA/miRNA* duplex, 5 nt; and flank sequence length of miRNA precursor, 10 nt. Finally, the identified miRNAs were predicted by Patmatch (v1.2) software. The minimum free energy (MFE) of the miRNA/target duplex was set at ≥ 74%; and there were no more than two adjacent mismatches in the miRNA/target duplex and no mismatches at positions 10–11 of the miRNA/target duplex.

Target gene function enrichment analysis

Blast2Go (Conesa et al. 2005) was employed to explore the Gene Ontology (GO) annotation terms. DAVID (Database for Annotation, Visualization and Integrated Discovery) was included to determine the pathways from the Kyoto Encyclopedia of Genes and Genomes (KEGG) database (Okuda et al. 2008). *P* values lower than 0.05 indicated enriched gene sets.

Verification of miRNAs and target genes by qRT-PCR

Candidate miRNA sequences were selected to quantitative real-time PCR (qRT-PCR) verification (Takara, Japan). qRT-PCR was conducted with the SYBR® PrimeScript™ miRNA RT-PCR Kit (RR716, Takara, China). Poly(A) tail addition and reverse transcription reactions were conducted in a total volume of 20 μL. The miRNA PrimeScript RT enzyme mix from the SYBR® PrimeScript™ miRNA RT-PCR Kit was used in the reverse transcription reaction mixtures, and the qRT-PCR primers used are listed in Table S1. Actin and U6 were adopted as internal control markers, and the relative expression of the miRNAs was calculated by the $2^{-\Delta\Delta Ct}$ method. All qRT-PCR tests were performed with three biological replicates.

Chlorophyll fluorescence measurement

The chlorophyll fluorescence induction kinetics were measured under a Fluocam (Photon System Instruments, Czech Republic) with a saturating flash intensity of ca. 2,000 μmol m^{-2} s^{-1}. The fluorescence intensity at 50 μs was regarded as the initial fluorescence, F_O; the maximum fluorescence level of the fluorescence transient was measured under saturating light. Before measurement of the chlorophyll fluorescence induction kinetics, the kelp sporophytes were adapted to the dark for 15 min to ensure complete oxidation of the PSII reaction centre.

Abbreviations

BF: biological process; bZIP: basic region/leucine zipper; ceRNAs: competing endogenous RNAs; LHC: light-harvesting complex; LHCSR3: light-harvesting complex stress-related protein 3; LOV: light-oxygen-voltage; miRNAs: microRNAs; MF: molecular function; NPQ: non-photochemical quenching; PAGE: polyacrylamide gel electrophoresis; PET: photosynthetic electron chain; PsbS:photosystem II subunit S; UVR8: ultra-violet resistance locus 8; WL: white light;

Declarations

Availability of data and materials

All supporting data can be found within the manuscript and its additional file. The datasets used during the current study are available from the corresponding author on reasonable request. We confirmed that we have included a statement regarding material availability in the declaration section of my manuscript.

Ethics approval and consent to participate

Not applicable.

Consent for publication

Not applicable.

Competing interests

The authors declare that they have a pending patent application based on the presented data.

Funding

This study was supported by the National Natural Science Foundation of China (31772848), Marine S &T Fund of Shandong Province for Pilot National Laboratory for Marine Science and Technology (Qingdao) (No. 2018SDKJ0502–1) and Joint Research Project Between China and Japan (No. 2017YFE0130900). The funding body had role in the collection, analysis, and interpretation of data.

Authors contributions

XQY has made substantial contributions to conception and design, or acquisition of data, or analysis and interpretation of data. DLD is involved in drafting the manuscript or revising it critically for important intellectual content.

Acknowledgement

The authors would like to thank Gene Denovo company (Guangzhou, China) for the technical supporting.

References

Allorent G, Lefebvrelegendre L, Chappuis R, Kuntz M, Truong T.B, Niyogi KK, Ulm R, Michel Goldschmidt-Clermont M (2017) UV-b photoreceptor-mediated protection of the photosynthetic machinery in *Chlamydomonas reinhardtii.* P Natl Acad Sci USA 113(51): 14864–14869

Bartel DP (2004) MicroRNAs: genomics, biogenesis, mechanism, and function. Cell 116(2):281–297

Chen YE, Liu WJ, Su YQ, Cui JM, Zhang ZW, Yuan M, Zhang H, Yuan S (2016) Different response of photosystem II to short and long-term drought stress in *Arabidopsis thaliana.* Physiol Plantarum 158(2):225–235

Cock JM, Liu FL, Duan DL, Bourdareau S, Lipinska AP, Coelho SM, Tarver JE (2017) Rapid evolution of microRNA loci in the brown algae. Genome Biol Evol 9(3):740–749

Cock JM, Sterck L, Rouzé P, Scornet D, Allen AE, Amoutzias G, Beszter B et al (2010) The *Ectocarpus* genome and the independent evolution of multicellularity in brown algae. Nature 465(7298):617

Costa BS, Sachse M, Jungandreas A, Bartulos CR, Gruber A, Jakob T, Kroth PG, Wilhelm C (2013) Aureochrome 1a is involved in the photoacclimation of the diatom *Phaeodactylum tricornutum.* PloS One 8(9):e74451

Conesa A, Götz S, García-Gómez JM, Terol J, Talón M, Robles M (2005) Blast2GO: a universal tool for annotation, visualization and analysis in functional genomics research. Bioinformatics 21(18): 3674–3676

Deng YY, Yao JT, Fu G, Guo H, Duan DL (2014) Isolation, expression, and characterization of blue light receptor aureochrome gene from *Saccharina japonica* (Laminariales, Phaeophyceae). Mar Biotechnol 16(2):135–143

Deng YY, Yao JT, Wang XL, Guo H, Duan DL (2012) Transcriptome sequencing and comparative analysis of *Saccharina japonica* (Laminariales, Phaeophyceae) under blue light induction. PloS One 7(6):e39704

Denzler R, Agarwal V, Stefano J, Bartel DP, Stoffel M (2014) Assessing the ceRNA hypothesis with quantitative measurements of miRNA and target abundance. Mol Cell 54(5):766–776

Gupta PK (2014) Competing endogenous RNA (ceRNA): a new class of RNA working as miRNA sponges.Curr Sci 106(6):823–830

Heijde M, Ulm R (2013) Reversion of the *Arabidopsis* uv-b photoreceptor uvr8 to the homodimeric ground state.P Natl Acad Sci USA 110(3):1113–1118

Jaubert M, Bouly JP, d'Alcalà MR, Falciatore A (2017) Light sensing and responses in marine microalgae. Curr Opin in Plant Biol 37:70–77

Jiao Y, Lau OS, Deng XW (2007) Light-regulated transcriptional networks in higher plants. Nat Rev Genet 8(3):217

Kawashima R, Sato R, Harada K, Masuda S (2017) Relative contributions of PGR5-and NDH-dependent photosystem I cyclic electron flow in the generation of a proton gradient in *Arabidopsis* chloroplasts. Planta 246(5):1045–1050

Luan HX, Yao JT, Chen ZH, Duan DL (2019) The 40S ribosomal protein S6 response to blue light by interaction with sjAUREO in *Saccharina japonica.*Int J Mol Sci 20(10):2414

Mann M, Serif M, Jakob T. Kroth PG, Wilhelm C (2017) Ptaureo1a and ptaureo1b knockout mutants of the diatom *Phaeodactylum tricornutum* are blocked in photoacclimation to blue light. J Plant Physiol 217

Matiiv AB, Chekunova EM (2018) Aureochromes–Blue Light Receptors. Biochemistry 83(6):662–673

Masuda S. Hasegawa K, Ohta H, Ono TA (2008) Crucial role in light signal transduction for the conserved Met93 of the BLUF protein PixD/Slr1694. Plant Cell Physiol 49(10):1600–1606

Nixon PJ, Mullineaux CW (2001) Regulation of photosynthetic electron transport. In Regulation of Photosynthesis, Kluwer Academic Publishers, Dordrecht, pp. 533–555

Okuda S, Yamada T, Hamajima M, Itoh M, Katayama T, Bork P, Kanehisa M et al (2008) KEGG Atlas mapping for global analysis of metabolic pathways. Nucleic Acids Res 36(suppl–2): W423-W426

Petroutsos D, Tokutsu R, Maruyama S, Flori S, Greiner A, Magneschi L et al (2016) A blue-light photoreceptor mediates the feedback regulation of photosynthesis. Nature 537(7621):563–566

Sato R, Kawashima R, Trinh M, Nakano M, Nagai T, Masuda S (2019) Significance of *pgr5*-dependent cyclic electron flow for optimizing the rate of *atp* synthesis and consumption in *Arabidopsis* chloroplasts. Photosynth Res 139(1–3):359–365

Song X, Li Y, Cao X, Qi Y (2019) MicroRNAs and their regulatory roles in plant-environment interactions. Annu Rev Plant Biol 70:489–525

Sun Z, Li M, Zhou Y, Guo T, Liu Y, Zhang H, Fang Y (2018) Coordinated regulation of *Arabidopsis* microRNA biogenesis and red light signaling through dicer-like 1 and phytochrome-interacting factor 4. PloS Genet 14(3):e1007247

Sun Y, Qiu Y, Duan M, Wang J, Zhang X, Wang H, Li X et al (2017) Identification of anthocyanin biosynthesis related microRNAs in a distinctive Chinese radish (*Raphanus sativus* L.) by high-throughput sequencing. Mol Genet Genomics 292(1):215–229

Takahashi F, Yamagata D, Ishikawa M, Fukamatsu Y, Ogura Y, Kasahara M et al (2007) Aureochrome, a photoreceptor required for photomorphogenesis in stramenopiles. P Natl Acad Sci USA 104(49): 19625–19630

Tarver JE, Cormier A, Pinzón N, Taylor RS, Carré W, Strittmatter M, Seitz H, Coelho SM, Cock JM (2015) microRNAs and the evolution of complex multicellularity: identification of a large, diverse complement of microRNAs in the brown alga *Ectocarpus.* Nucleic Acids Res 43(13):6384–6398

Voinnet O (2009) Origin, biogenesis, and activity of plant microRNAs. Cell 136(4):669–687

Wang WJ, Sun XT, Wang GC, Xu P, Wang XY, Lin ZL, Wang FJ (2010) Effect of blue light on indoor seedling culture of *Saccharina japonica* (Phaeophyta). J Appl Phycol 22(6):737–744

Tables

Table 1 Integrated microRNA and mRNA expression profiling revealed the potential miRNAs that targeted to aureochrome.

miRNA	Description	hairpin_energe(kcal/mol)	MFE ratio	target_region(3'->5')	mirna-target_pairing(5'->3')	miRNA_sequence(5'->3')
novel-m1387-5p	aureochrome1	-22.3	0.6282	GUUCAUCACACAGGGUUUUU	|||||||x|||||x||x|	CAAGUAGUUUGUCCCCAACA
novel-m0501-5p	aureochrome1	-33.2	0.7297	AGCACAGAGCGGGGAGCCGG	|||x|||||||oxo||||	UCGAGUCUCGCCCUGUGGCC
novel-m1387-3p	aureochrome 1	-27.4	0.7697	CACCCCUGCUUUGUGAACCU	x||||||x||oo|||||	UUGGGGACAAAAUGCUUGGA
novel-m2470-5p	aureochrome 1	-39.8	0.8257	GACGACGACGACGACGACCGA	||||||x|||||||||ox	CUGCUGCCGCUGCUGCUGGUC
novel-m2470-5p	aureochrome 1	-41.9	0.8747	GACGACUGCGACGACGACGAA	|||||x||||||||x|x	CUGCUGCCGCUGCUGCUGGUC
novel-m2470-5p	aureochrome 1	-40.8	0.8518	GGCGACGGCGACGACGACGGC	|o||||||||||||xox	CUGCUGCCGCUGCUGCUGGUC
novel-m3443-3p	aureochrome 1	-42	0.8861	CGACGACGACGACGACGACCG	|||||||||||||x|x	GCUGCUGCUGCUGCUGCUAGG
novel-m3461-5p	aureochrome 1	-25.1	0.7382	CACCCCUGCUUUGUGAACCUU	x|||||x||x||||||	UUGGGGACAAAAAACUUGGAA
novel-m3833-3p	aureochrome 1	-27.4	0.7697	CACCCCUGCUUUGUGAACCU	x|||||x||oo|||||	UUGGGGACAAAAUGCUUGGA
novel-m3940-3p	aureochrome 1	-41.6	0.8889	GACGACGACGACGACGACCGA	|||||||||||||x|xx	CUGCUGCUGCUGCUGCUAGGC
novel-m4067-3p	aureochrome 1	-25.2	0.6942	AGGUUUGGGAGGAGCUAACGG	|||||x|||x|||||xo|	UCCAAACGCUCGUCGAUUUUC
novel-m4476-3p	aureochrome 1 [Ectocarpus siliculosus]	-31.6	0.7435	AAGGCGGCGGCGGCGAUGACU	|||xo|||||x|||||x	UUCCUUCGCCGCAGCUACUGU
novel-m5041-5p	aureochrome 1	-42	0.8861	CGACGACGACGACGACGACCG	|||||||||||||x|x	GCUGCUGCUGCUGCUGCUAGG
novel-m5132-3p	aureochrome 1	-39.8	0.8257	GACGACGACGACGACGACCGA	||||||x|||||||||ox	CUGCUGCCGCUGCUGCUGGUC
novel-m5132-3p	aureochrome 1	-41.9	0.8747	GACGACUGCGACGACGACGAA	|||||x||||||||x|x	CUGCUGCCGCUGCUGCUGGUC
novel-m6643-3p	aureochrome 1	-42	0.8861	CGACGACGACGACGACGACCG	|||||||||||||x|x	GCUGCUGCUGCUGCUGCUAGG
novel-m3150-5p	aureochrome2	-29.4	0.7119	UCGUGGACCAGCUCGCACAUGG	||||x|||||||x|x||x	AGCACGUGGUCGAGCAUUUACG
novel-m3151-5p	aureochrome2	-29.4	0.7119	UCGUGGACCAGCUCGCACAUGG	||||x|||||||x|x||x	AGCACGUGGUCGAGCAUUUACG
miR8181-x	aureochrome 5	-33.1	0.7088	CAUCCCUCCCCGCCACGG	|xo||||||x|||x|	GGGGGGAGGGGGGGUGAC
miR8181-x	aureochrome 5	-38.6	0.8319	CUCCCCCCCCCCCCCGCUG	|o|||x||||||o|||	GGGGGGAGGGGGGGUGAC
novel-m2866-5p	aureochrome 5	-34.4	0.8329	ACCUUCGAAGCGCUUGAGGA	xx||||||||||o||||	CUGAAGCUUCGCGAGCUCCU
novel-m4645-3p	aureochrome 5	-36	0.7965	GUCGUGGUAGAGGAGGUCGGG	|x||x||||||||||oo|	CCGCUCCAUCUCCUCCAGUUC

Table 2 Analysis of negative regulatory miRNA and *Aureochrome5* expression.

miR_ID	target	cor	*P*-value
miR8181-x	*Aureochrome 5*	-0.654653671	0.158302423
novel-m2866-5p	*Aureochrome 5*	-0.771428571	0.072396501

Figures

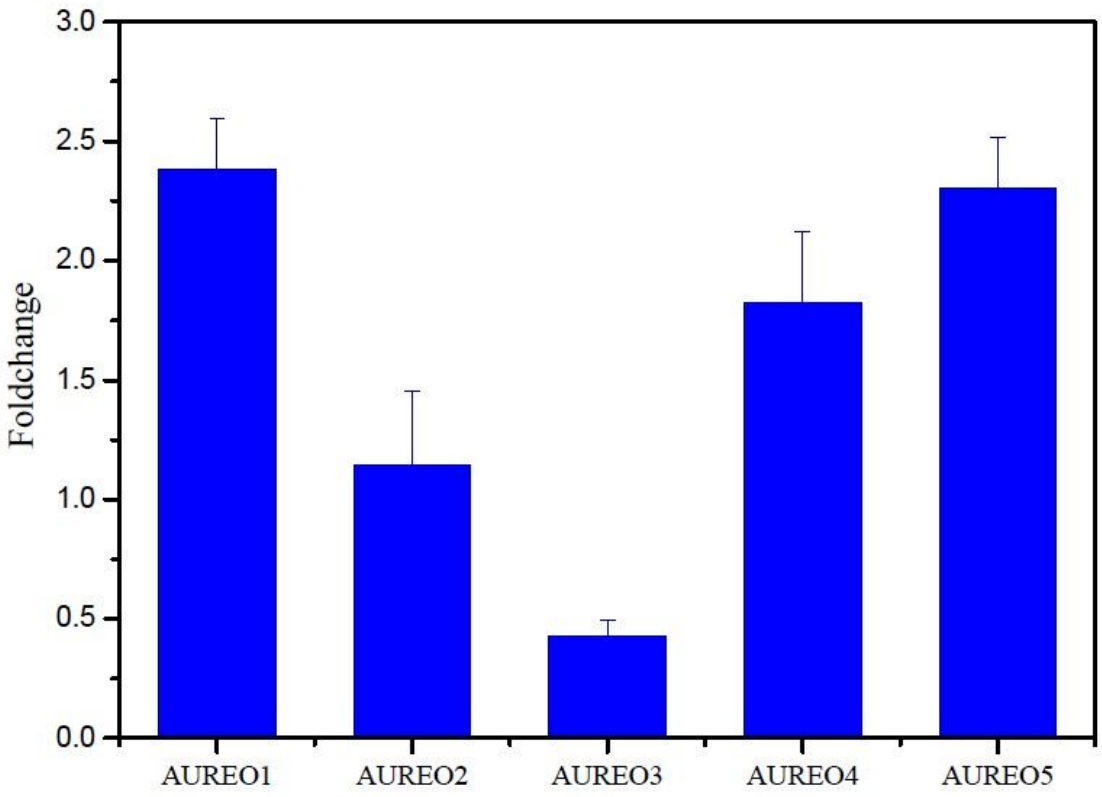

Figure 1

Relative expression profiles of five Aureochrome homologs transcripts in response to blue light. Values are normalized for β-actin expression levels and represent means ± S.E. for n = 3.

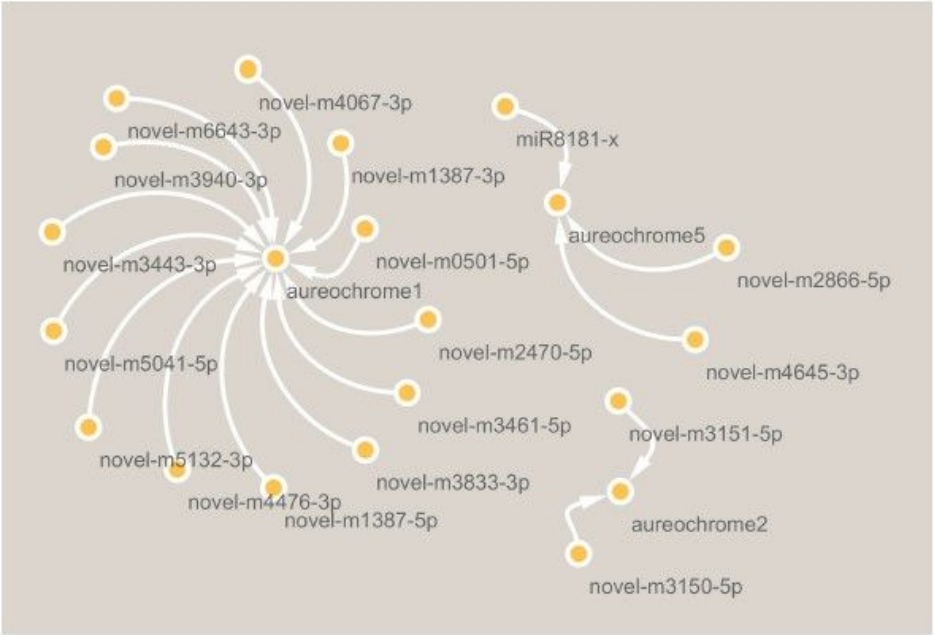

Figure 2

The regulatory network between miRNAs and Aureochrome homologs.

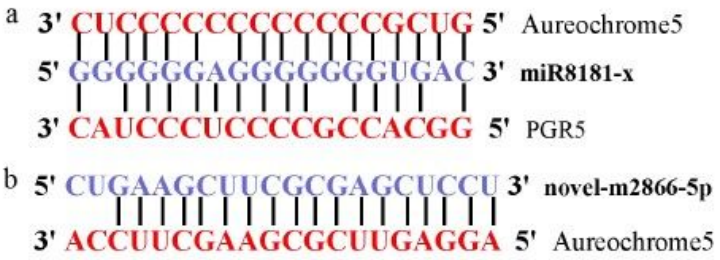

Figure 3

Base-pairing interaction between miRNAs and Aureochrome5.

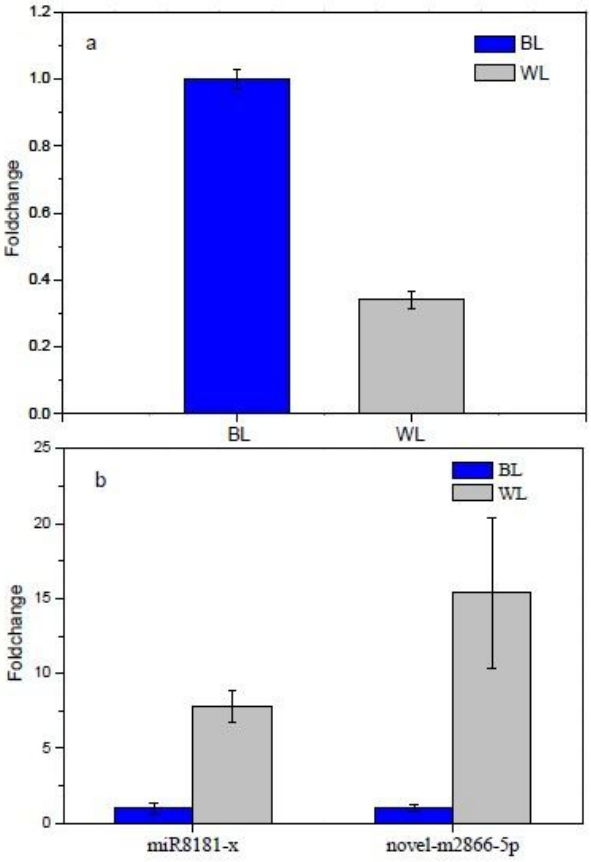

Figure 4

qRT-PCR analyses of Aureochrome5 (a), miR8181-x, and novel-m2866-5p (b) transcripts in response to blue light (jewelry blue) and white light (light grey). Values are normalized for β-actin expression levels and represent means ± S.E. for n = 3.

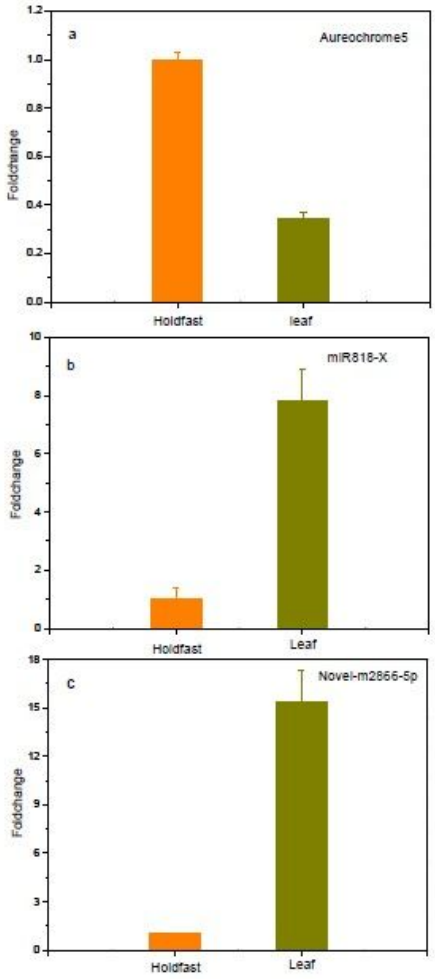

Figure 5

Relative expression profiles of Aureochrome5 (a), miR8181-x (b), and novel-m2866-5p (c) transcripts in different tissues. Values are normalized for β-actin expression levels and represent means ± S.E. for n = 3.

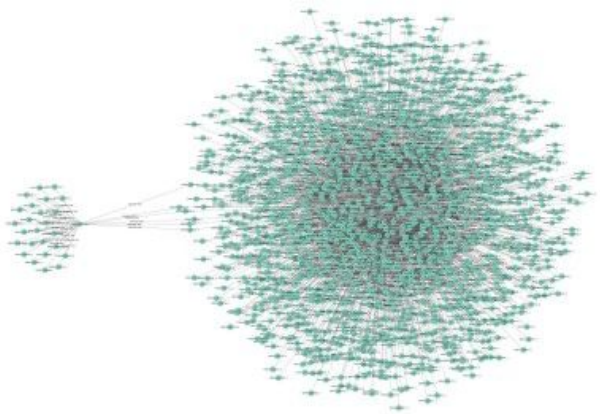

Figure 6

The regulatory network between miRNAs and target genes.

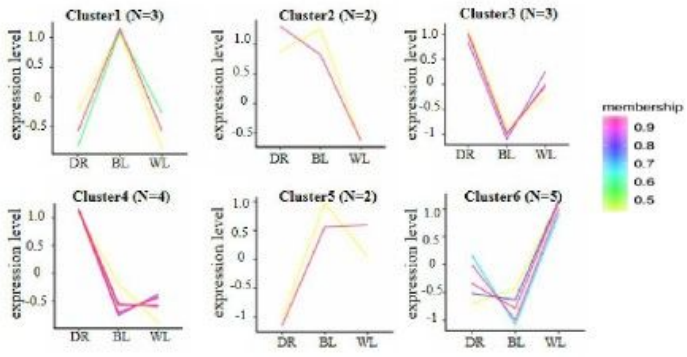

Figure 7

A set of diagrams showing six patterns of dynamic expression in the target genes of novel-m2866-5p in response to different light treatments.

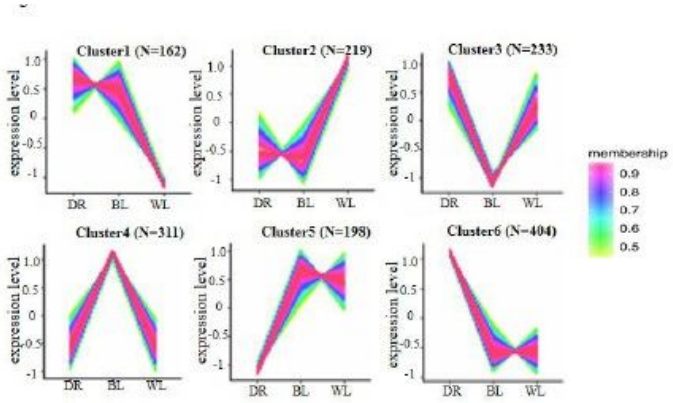

Figure 8

A set of diagrams showing six patterns of dynamic expression in the target genes of miR-8181-x in response to different light treatments.

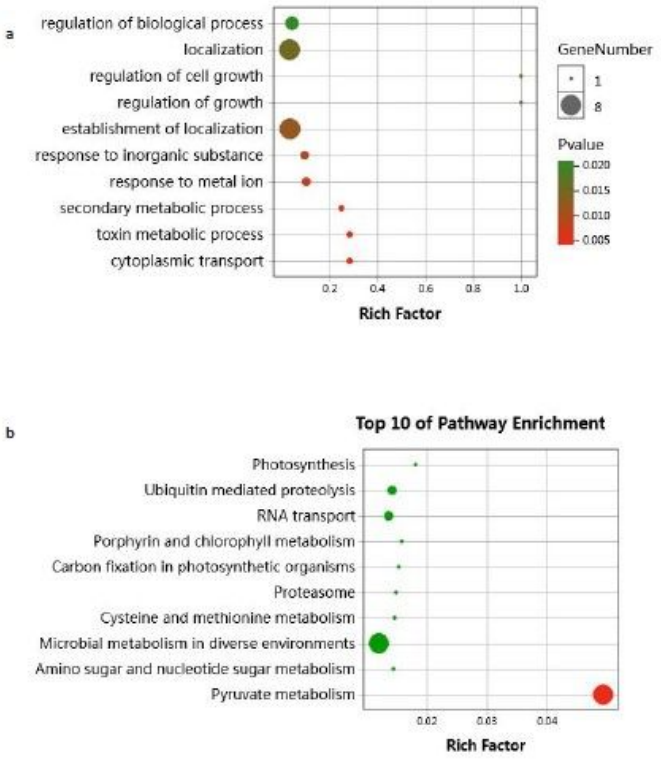

Figure 9

9 GO annotations of cluster4 target genes of miR-8181-x with the top 10 enrichment scores of biological processes (a). Enrichment analysis of KEGG pathways of cluster4 target genes of miR8181-x with the top 10 enrichment scores of biological processes (b). The gradual color represents the P value; the size of the spot represents the gene number.

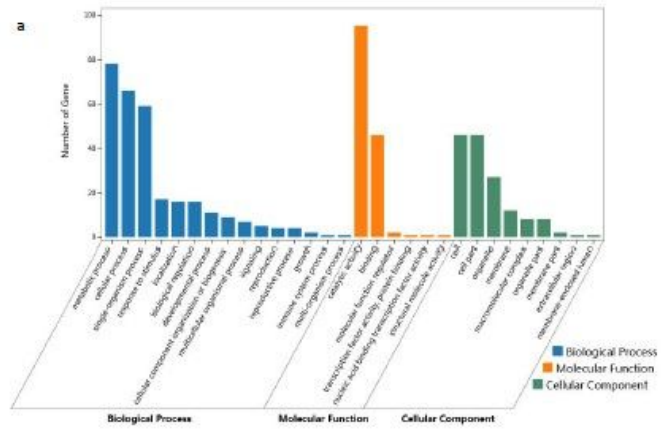

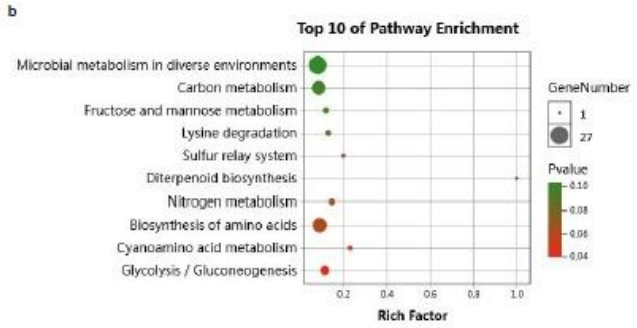

Figure 10

Analysis of miR-8181-x function. Go analysis (a) and KEGG pathway analysis (b) for the target genes of miR-8181-x.

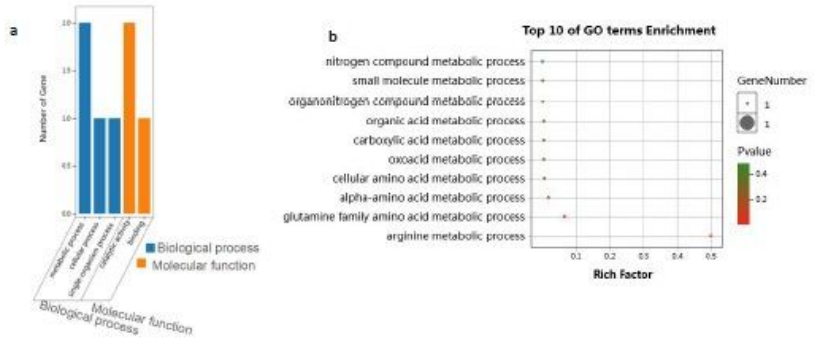

Figure 11

Analysis of novel-m2866-5p function. Go analysis (a) and KEGG pathway 38 analysis (b) for the target genes of novel-m2866-5p.

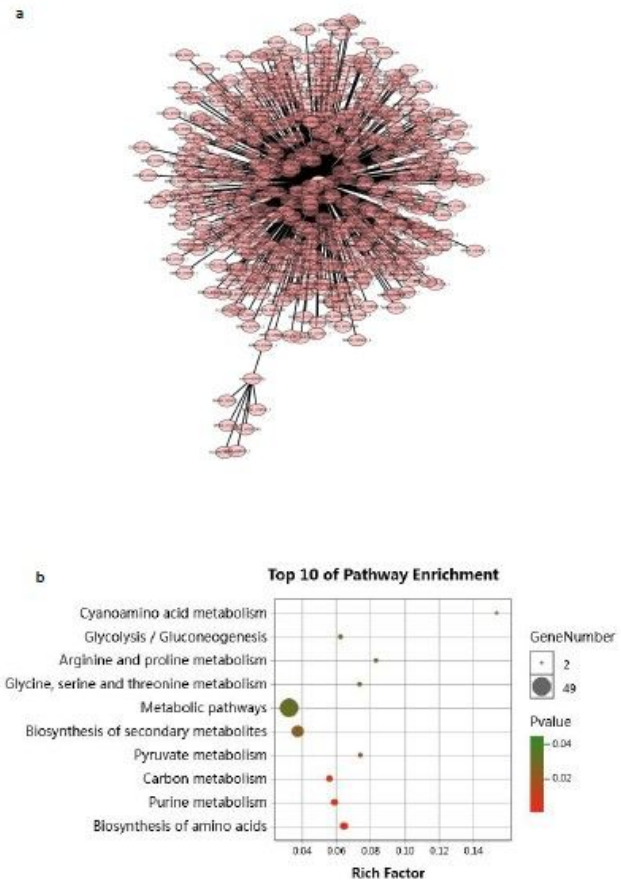

Figure 12

Analysis of the regulatory function of Aureochrome5. (a) The potential ceRNAs of Aureochrome5 that exhibited negative correlation with novel-m2866-5p and miR8181-x. (b) KEGG pathway analysis for the ceRNAs.

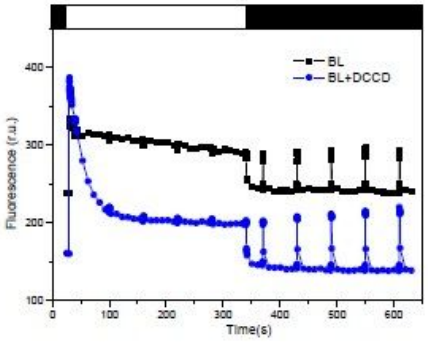

Figure 13

The effect of DCCD incubation on the chlorophyll a fluorescence dynamics. The protocol included a dark preadaptation period of 5 min, a period of strong light (white bar; 5 min; 750 μmol·m−2·s−1) followed by a period of relaxation in the dark (black bar; 5 min). The fluorescence dynamics in response to blue light was set as control (black lines).

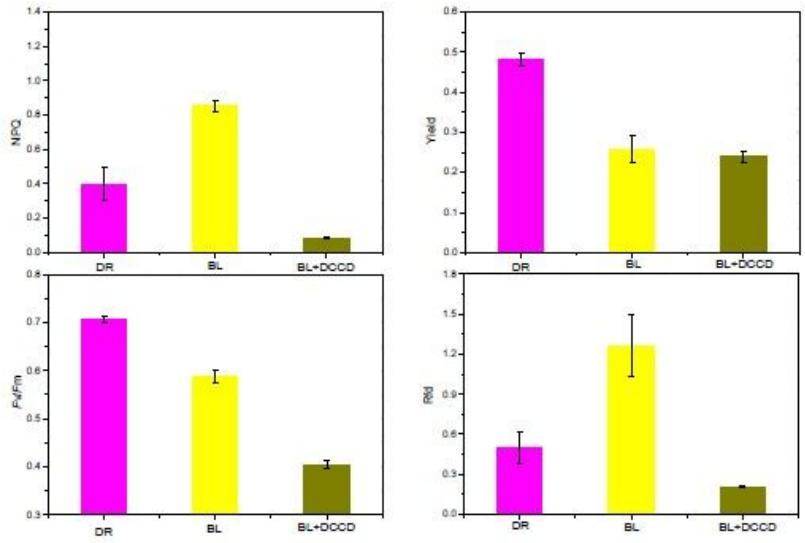

Figure 14

The effect of DCCD incubation on the NPQ (a), Yield (b), Fv/Fm (c) and Rfd (d) of Saccharina 48 japonica in response to blue light.

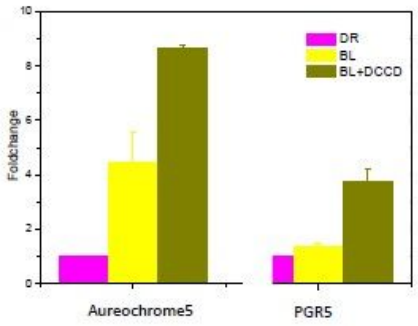

Figure 15

The effect of DCCD incubation on the expression of Aureochrome5 and PGR5. qRT-PCR analyses of Aureochrome5 and PGR5 transcripts in response to blue (tulip yellow) and blue+DCCD (olive green) treatment. Values are normalized for b-actin expression levels and represent means ± S.E. for n = 3.

Supplementary Files

This is a list of supplementary files associated with this preprint. Click to download.

- Suppletarymaterials.doc